RELAX: Detecting Relaxed Selection in a Phylogenetic Framework

Joel O. Wertheim,*[,1] Ben Murrell,[1] Martin D. Smith,[2] Sergei L. Kosakovsky Pond,[1] and Konrad Scheffler*[,1,3]

[1]Department of Medicine, University of California, San Diego

[2]Bioinformatics and Systems Biology Graduate Program, University of California, San Diego

[3]Department of Mathematical Sciences, Stellenbosch University, Stellenbosch, South Africa

***Corresponding author:** E-mail: jwertheim@ucsd.edu; kscheffler@ucsd.edu.

Associate editor: Beth Shapiro

Abstract

Relaxation of selective strength, manifested as a reduction in the efficiency or intensity of natural selection, can drive evolutionary innovation and presage lineage extinction or loss of function. Mechanisms through which selection can be relaxed range from the removal of an existing selective constraint to a reduction in effective population size. Standard methods for estimating the strength and extent of purifying or positive selection from molecular sequence data are not suitable for detecting relaxed selection, because they lack power and can mistake an increase in the intensity of positive selection for relaxation of both purifying and positive selection. Here, we present a general hypothesis testing framework (RELAX) for detecting relaxed selection in a codon-based phylogenetic framework. Given two subsets of branches in a phylogeny, RELAX can determine whether selective strength was relaxed or intensified in one of these subsets relative to the other. We establish the validity of our test via simulations and show that it can distinguish between increased positive selection and a relaxation of selective strength. We also demonstrate the power of RELAX in a variety of biological scenarios where relaxation of selection has been hypothesized or demonstrated previously. We find that obligate and facultative γ-proteobacteria endosymbionts of insects are under relaxed selection compared with their free-living relatives and obligate endosymbionts are under relaxed selection compared with facultative endosymbionts. Selective strength is also relaxed in asexual *Daphnia pulex* lineages, compared with sexual lineages. Endogenous, nonfunctional, bornavirus-like elements are found to be under relaxed selection compared with exogenous Borna viruses. Finally, selection on the short-wavelength sensitive, *SWS1*, opsin genes in echolocating and nonecholocating bats is relaxed only in lineages in which this gene underwent pseudogenization; however, selection on the functional medium/long-wavelength sensitive opsin, *M/LWS1*, is found to be relaxed in all echolocating bats compared with nonecholocating bats.

Key words: **relaxed selection, molecular evolution, codon models, phylogenetics, endosymbionts, echolocation, opsin, *Daphnia pulex*, bornavirus.**

Article

Introduction

The essential role of natural selection in shaping organismal diversity and enabling evolutionary innovation is a fundamental tenet of modern biology (Lenski et al. 2003; Holmes and Drummond 2007). Genes, lineages, or genomic sites that are conserved by natural selection are important for preserving function (Graur et al. 2013), whereas some changes may confer adaptive advantage (Eyre-Walker 2006; Elde and Malik 2009). A dizzying array of phylogenetic techniques for identifying targets of natural selection is available to researchers, following close to 30 years of development (Anisimova and Kosiol 2009; Delport et al. 2009). Nearly all phylogenetic methods in use today estimate the ratio of nonsynonymous to synonymous substitution rates (ω or dN/dS) and test for significant deviations from the neutral expectation of $\omega = 1$.

The understandable focus on identifying instances of strong selection has created a methodological gap concerning biologically interesting cases when the absence or reduction in efficiency of natural selection is important. For example, relaxed selection—a gene-wide or genome-wide reduction in the efficiency or intensity of both purifying and positive selection—can allow for an exploration of a wider subset of the phenotypic space and foster evolutionary innovation (Lahti et al. 2009; Snell-Rood et al. 2010; Hunt et al. 2011). Selection can be relaxed in a variety of ways, including the removal of a functional constraint (e.g., a new ecological niche) or the reduction in efficiency of selection (e.g., increased relevance of genetic drift due to a reduction in effective population size). After gene duplication, neofunctionalization and subfunctionalization may be facilitated by relaxation of selective constraints, followed by positive selection for previously inaccessible features (Ohno 1970; Lynch and Conery 2000). Conversely, relaxed selection can also lead to gene loss through pseudogenization (Wu et al. 1986; Go et al. 2005). Relaxed selection has also been implicated as both a driver of speciation (Templeton 2008) and a precursor to extinction (Moran 1996).

A number of ad hoc approaches have been used to look for evidence of relaxed selection. The most obvious approach has been to identify loss of trait or pseudogenization (e.g., Dainat et al. [2012]). This approach detects the terminal effects of relaxation, but it is not capable of detecting subtler changes in the intensity of selection that may not drive a gene to obsolescence or cause a loss of function. In the context of comparative phylogenetic analysis, existing ω-based methods designed to look for deviations from neutrality have been shoehorned into seeking evidence for neutrality. A popular test for relaxed selection, based on the partitioned lineages model of Bielawski and Yang (2003), divides all branches into groups *a priori* and estimates a single ω within each group (Zhao, Ru, et al. 2009; Veilleux et al. 2013; Feng et al. 2014; Marková et al. 2014; Wicke et al. 2014). A higher ω within a group is interpreted as evidence for relaxation of selective constraints, as those constraints tend to reduce the rate of nonsynonymous substitutions relative to that of synonymous substitutions, thereby keeping ω values low. However, this test can be misleading because estimates of ω can be increased by processes such as intensification of positive selection when selective pressures vary both along branches and sites (Murrell et al. 2012).

Relaxed selection across sites in a gene has also been explored by estimating the number of sites under strong purifying selection in one region versus another (Wertheim and Worobey 2009) and by directly testing for differences in site-specific ω estimates (Pond et al. 2006); however, such approaches are relevant primarily for comparing selective pressures across regions within a gene. In contrast, our interest in this study is in comparing gene-wide selection intensity across branches.

We present a formal hypothesis test for relaxed selection: RELAX. It builds upon the random effects branch-site (BS-REL) models (Kosakovsky Pond et al. 2011), which were developed to overcome statistical and methodological restrictions imposed by the popular "branch-site" class of evolutionary models (Yang and Nielsen 2002). In a BS-REL framework, the ω ratio along each branch at a given site is drawn from a discrete distribution of ω values independently of other branches in the tree, affording RELAX a flexible and powerful mechanism for handling heterogeneous selective pressures. We validate the performance of RELAX using simulations as well as four biological examples where relaxation would be expected according to evolutionary theory: 1) endosymbiosis in γ-proteobacteria, 2) color vision genes in bats, 3) viral endogenization in bornaviruses, and 4) asexual reproduction in crustaceans.

New Approaches

Historical Context

The first codon models estimated parameters representing an averaged nonsynonymous–synonymous rate ratio. This average could be estimated across all branches and sites (Goldman and Yang 1994) or for individual branches but still averaged across all sites (Muse and Gaut 1994). Such gene-wide average ω values were typically below 1, because most sites in protein-coding genes are strongly conserved. The introduction of site-to-site rate variation allowed detection of individual sites evolving under positive selection, by classifying sites into different rate categories and estimating a separate ω value specifically for the sites in the positive selection category (Nielsen and Yang 1998). This approach led to the detection of sites for which ω is well above 1, even in genes where the average ω value estimated across all sites is below 1. Therefore, it became conventional to think in terms of the distribution of ω values over sites instead of a single gene-wide ω (Yang et al. 2000). An ω distribution can be thought of as an evolutionary fingerprint characterizing the evolutionary pattern of the gene, where a small subset of sites can have very large ω values even when the majority of sites evolved under strong purifying selection (Kosakovsky Pond, Scheffler, et al. 2010). This approach contrasts with simpler mean ω models in which all sites are described by a single ω value.

When rate variation over time is not modeled, ω values for specific sites or site categories represent time-averages over all branches in the phylogeny. The introduction of branch-site models addressed evolutionary rate variation not only over sites but also over branches (Yang and Nielsen 2002). Our random effects (Kosakovsky Pond et al. 2011) and mixed effects (Murrell et al. 2012) branch-site models allow detection of individual branches on which only a subset of sites are under positive selection or, conversely, individual sites which are under positive selection on only a subset of branches. The change from phylogeny-level resolution to branch-level resolution yielded higher branch-specific ω values than phylogeny-wide ω values, mirroring the effect obtained when site-to-site rate variation was introduced. This development vastly increased the detectable instances of positive selection (Murrell et al. 2012).

In this study, we are interested in time-heterogeneous situations where the evolutionary fingerprint (the distribution of ω values over sites) differs between one part of the phylogeny and another. Such variation across the phylogeny can be studied using the BS-REL model (Kosakovsky Pond et al. 2011). For every branch or set of branches of interest, one can estimated a separate ω distribution over sites. Below we introduce a variant of this model that can determine whether the ω distribution inferred for one part of the phylogeny represents selective relaxation or intensification relative to another part of the phylogeny.

General Model Overview

Our test for relaxed selection is based on the different effects relaxation has on ω values smaller than 1, representing purifying selection, and on ω values larger than 1, representing positive selection. When selection is relaxed, the smaller ω values increase toward 1, whereas ω values above 1 decrease. In the context of branch-site models with multiple ω categories represented by different proportions of sites, this trend can have two different effects: The ω values inferred for the selection categories can move toward 1 (fig. 1) and/or the proportions of sites belonging to the different categories can

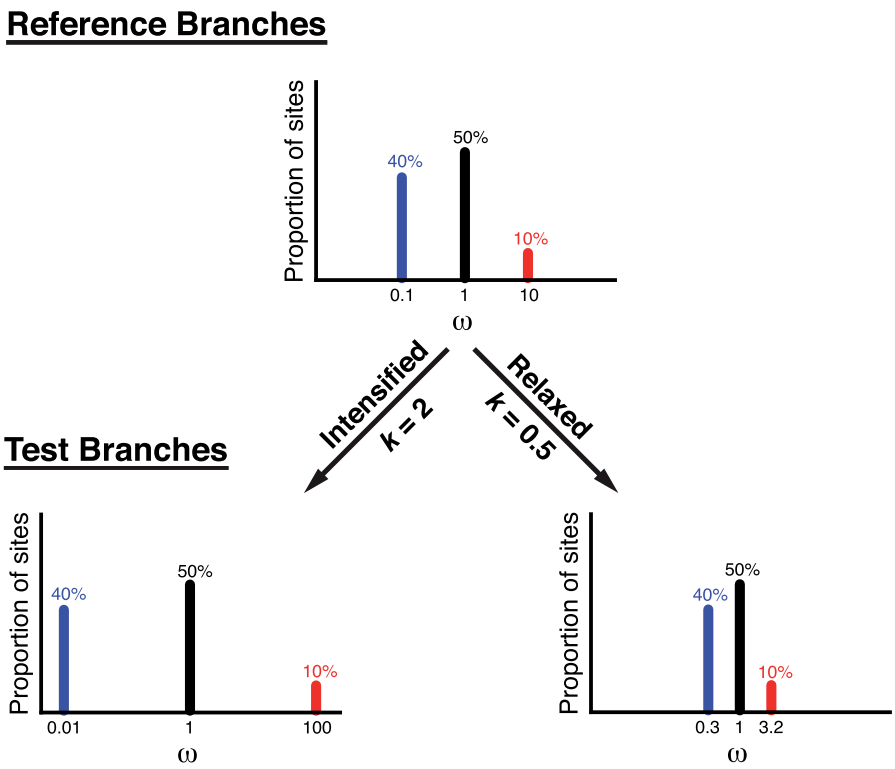

Fig. 1. Modeled effects of intensified and relaxed selection. Intensified selection pushes all ω categories away from neutrality ($\omega = 1$), whereas relaxed selection pushes all ω categories toward neutrality ($\omega = 1$). Sites under purifying selection are shown in blue and sites under positive selection in red. See Materials and Methods for a definition of the selection intensity parameter k.

change in such a way that more sites are assigned to categories with ω values closer to 1.

Consider a phylogenetic tree τ, in which all branches are partitioned *a priori* into disjoint sets: test branches (T), reference branches (R), and unclassified branches (U). The U class may be empty, but both T and R contain at least one branch each. The idea of RELAX is to use the BS-REL framework estimate a separate discrete distribution of ω for each of these branch classes and compare them. To develop a simple hypothesis test for relaxed selection, we further reduce the complexity of the BS-REL model by enforcing the constraint that $\omega_T = \omega_R^k$, so that each ω component of the test distribution is obtained by raising the corresponding component of the reference distribution to the power k. We term the exponent $k \geq 0$ the selection intensity parameter (see detailed model description below). We then perform a likelihood ratio test (LRT) by comparing the null model in which k is constrained to 1 (i.e., the same ω distribution on test and reference branches) to an alternative model in which k is a free parameter. When the introduction of k produces a statistically significant improvement in model fit, we conclude that selection on test branches is intensified ($k > 1$) or relaxed ($k < 1$) compared with background branches.

Qualitatively, the selection intensity parameter will modulate the degree to which different ω classes diverge from neutrality ($\omega = 1$) in the test branches versus the reference branches (fig. 1). Under intensified selection (e.g., $k = 2$), sites under moderate purifying selection in the reference branches become subjected to stronger purifying selection in the test branches ($\omega = 0.1$ shifting to $\omega = 0.01$; shown in blue in fig. 1). Likewise, sites under moderate positive selection in the reference branches become subjected to stronger positive selection in the test branches ($\omega = 10$ shifting to $\omega = 100$; shown in red in fig. 1). In contrast, under relaxed selective strength (e.g., $k = 0.5$), sites under moderate purifying selection in the reference branches become subjected to weaker purifying selection in the test branches ($\omega = 0.1$ shifting to $\omega = 0.3$; shown in blue in fig. 1). Likewise, sites under moderate positive selection in the reference branches become subjected to weaker positive selection in the test branches ($\omega = 10$ shifting to $\omega = 3.2$; shown in red in fig. 1).

Detailed Model Description

There are many different ways to shrink or expand the ω distribution. We chose the parametric form $f(\omega, k) = \omega^k$ guided by the requirements that it should:

- have a single parameter k corresponding to "intensity" [i.e., $\forall \omega \geq 0 : f(\omega, k)$ is monotonic in k], with low values of k shrinking $f(\omega, k)$ toward 1 and high values of k expanding it away from 1,
- be nonnegative ($\forall k, \omega \geq 0 : f(\omega, k) > 0$),
- have a unique value of k corresponding to no relaxation or intensification; for our chosen parametric form the value is $k = 1$, giving $\forall \omega \geq 0 : f(\omega, 1) = \omega$.

In logarithmic space, the mapping is linear [i.e., $\log f(k, \omega) = k \log \omega$]. We note that RELAX could trivially

accommodate other parametric forms of the ω transformation.

The evolutionary process is described by a three-category BS-REL model, which is an extension of the standard codon-substitution model structure, with explicit dependence of the ω ratio on the specific branch $b \in \{1, \ldots, B\}$ and the rate class $c \in \{1, 2, 3\}$. The (i, j) entry of the instantaneous rate matrix $Q_{b,c}$, describing the rate at which codon i is replaced with codon j, is given by:

$$q_{ij}(b, c, k_b, \theta, \Pi) = \begin{cases} \theta_{ij}\pi_j, & \delta(i,j) = 1, AA(i) = AA(j), \\ \omega_{b,c}^{k_b}\theta_{ij}\pi_j, & \delta(i,j) = 1, AA(i) \neq AA(j), \\ 0, & \delta(i,j) > 1, \\ -\sum_{l \neq i} q_{il}, & i = j. \end{cases} \quad (1)$$

Here, $\delta(i, j)$ counts the number of nucleotide differences between codons i and j; $AA(x)$ is the amino acid encoded by codon x; θ represents the underlying nucleotide substitution rate parameters (assumed to follow the general time reversible [GTR] form); Π are the equilibrium codon frequencies, obtained using the CF3x4 corrected empirical estimator (Kosakovsky Pond, Delport, et al. 2010) with nine parameters; $\omega_{b,c}$ ($\omega_{b,1} \leq \omega_{b,2} \leq 1 \leq \omega_{b,3}$) is the nonsynonymous/synonymous rate ratio value associated with branch b and category c; and k_b is the branch-dependent selection intensity parameter.

For each branch b, we also define a set of weight parameters $p_{b,c}$ corresponding to the three categories, such that $\sum_{c=1}^{3} p_{b,c} = 1$. The likelihood of the data d_s at a single codon site s for a given vector of estimable model parameters, Θ, is computed by marginalizing over all possible assignments of categories to branches. Formally, let C be the ω−configuration vector of length B, where each entry C_b is an integer in 1, 2, 3, representing the statement that ω at branch b takes the corresponding value from the discrete distribution of ω values at that branch. Then, modeling the probability of any particular configuration as the product of individual branch weights ($P(C) = \prod_{b=1}^{B} p_{b,C_b}$),

$$P(d_s \mid \Theta) = \sum_{C} P(d_s \mid C, \Theta)P(C), \quad (2)$$

where the sum is over 3^B potential ω-configurations. We have previously shown (Kosakovsky Pond et al. 2011) that this sum can be computed efficiently using Felsenstein's pruning algorithm (Felsenstein 1981) with the transition probability matrix operating on branch b (with branch length t_b) given by a weighted sum of the three transition probability matrices:

$$P(b, t_b) = \sum_{c=1}^{3} p_{b,c} e^{Q_{b,c} t_b}. \quad (3)$$

Finally, the overall likelihood of the alignment is the product of constituent site likelihoods under the standard assumption of independence. All model parameters are estimated by maximum likelihood, except for codon frequency parameters, which are obtained from nucleotide counts (Kosakovsky Pond, Delport, et al. 2010).

The above description provides a general framework which has $14 + B$ baseline parameters: 5 nt rate parameters θ, 9 frequency parameters defining the codon frequencies Π, and B branch lengths t_b. Parameters governing the ω distribution can be added to obtain a series of special cases of this framework (described below and in fig. 2).

A Hypothesis Test for Relaxation or Intensification of Selection

To test whether or not selection is relaxed (or intensified) on the subset of test branches T relative to the subset of reference branches R, we define a pair of null and alternative models (fig. 2) using a single three-category distribution of ω (comprising three selection parameters ω_c and their corresponding weight parameters p_c, of which two are independent) that is shared by all branches in T and R. If there are unclassified branches in the tree, we define a separate distribution of ω shared by all such branches. In the null model, the selection intensity parameter is set to 1 for all branches, thereby recapitulating the standard BS-REL model. In the alternative model, all branches in the test T set share a single selection intensity parameter, k. We perform a LRT using the standard χ^2 asymptotic distribution with 1 degree of freedom to determine significance: If the null model is rejected by the LRT, it indicates that selection on the test branches is intensified ($k > 1$) or relaxed ($k < 1$) compared with the reference branches.

Descriptive Analysis of Selection Profiles on the Reference and Test Branch Sets

When the aim is to produce a quantitative description of the selection patterns in test and reference branches, regardless of whether these patterns are significantly different from each other, we use a less constrained Partitioned Descriptive model (fig. 2) in which separate distributions of ω are estimated for branch sets T and R instead of using the selection intensity parameter. We implemented this model as a means to describe the data and to provide a goodness-of-fit reference for the hypothesis testing framework.

Descriptive Analysis of Selective Constraints without A Priori Partitioning

Finally, we implemented the *General Descriptive* model (fig. 2), wherein the underlying selective regime is described as a single ω distribution shared by all the branches, but each branch either relaxes or intensifies the "average" selective regime via its own k_b parameter. To ensure identifiability, we fix the geometric mean of the ω distribution to 1. The ω values in the rate matrices are still adjustable via the k_b parameter for that branch, so this constraint does not involve loss of model generality. We use this model to visualize the variation in relative selective constraint across the tree without an *a priori* partitioning of branches. If there are no

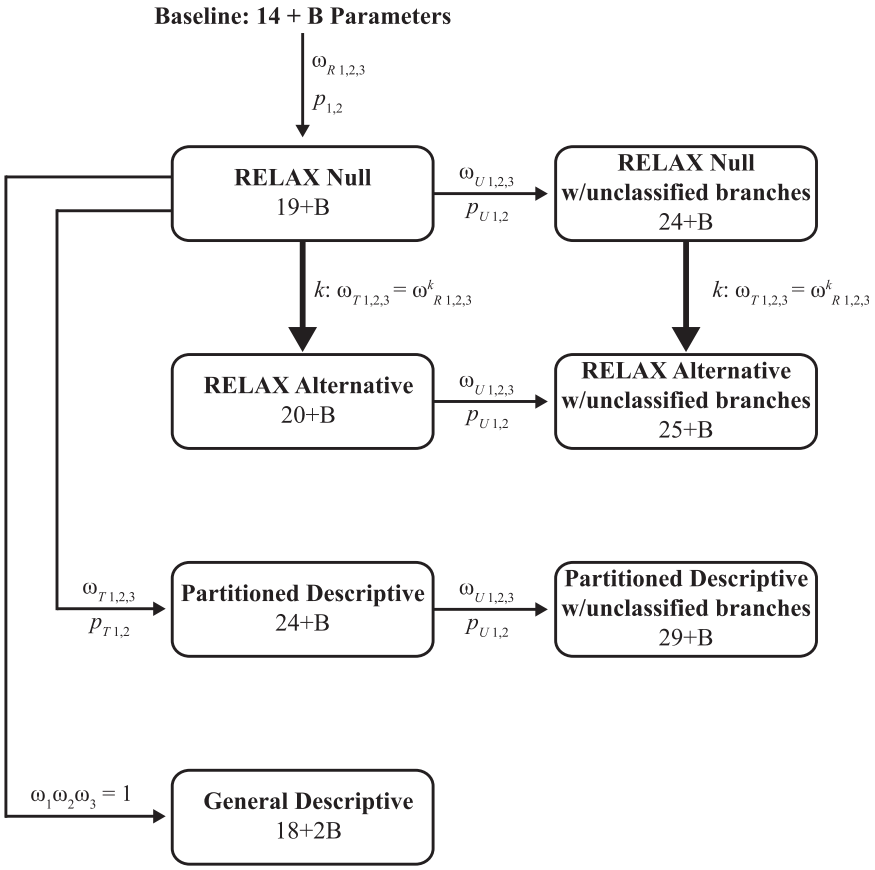

Fig. 2. The relationships among models used by RELAX. Models are shown in boxes, with the number of estimable parameters indicated below the model name. Arrows indicate parameters added to related models. Parameters ω, p, and k are shared by groups of branches. For a tree with B branches, all models have $14 + B$ baseline parameters: 5 nt rate parameters θ, and nine frequency parameters defining the codon frequencies Π, and B branch lengths t_b. The bold arrows indicate the hypothesis test in RELAX.

unclassified branches, this model is a superset of the RELAX null and alternative models.

Simulations

Three sets of simulations were performed to assess the validity of RELAX. The first simulation investigated the type I error rate. We generated 1,000 codon alignments over the γ-proteobacteria phylogeny. We simulated codon evolution under the parameter values inferred under the RELAX null model (fig. 2), but constraining ω_3 to be no larger than 10. We enforced this constraint due to the flat likelihood surface associated with high ω values, which makes the larger empirical estimate for this parameter unreliable. The constraint on ω_3 resulted in slightly higher estimates for ω_1 and ω_2, which we used for this simulation:

$\omega_1 = 0.02\,(p_1 = 0.82)$, $\omega_2 = 0.38\,(p_2 = 0.17)$, $\omega_3 = 10$ $(p_3 = 0.01)$. The selection intensity parameter k was fixed to 1.

To evaluate the statistical power of RELAX, we again performed simulations over the the γ-proteobacteria phylogeny. Primary and secondary endosymbiont branches were classified as test branches T and non-endosymbiont branches were classified as reference branches R. Three selection scenarios were considered for R, with ω distributions ranging from mildly diffuse to highly diffuse (see fig. 4 for parameter details). For each selection scenario, selection on the T branches was modulated by 1 of 11 k values ranging between 0 and 1. For each k value in each selection scenario, 100 replicates were generated.

We also investigated the robustness of RELAX to the effect of increasing only the selection intensity of positive selection in a subset of branches (i.e., model misspecification). We simulated 100 replicates over a four-taxon phylogeny (fig. 3). Along three of the five branches, the following selective regime was used: $\omega_1 = 0.01\,(p_1 = 0.5)$, $\omega_2 = 1\,(p_2 = 0.35)$, $\omega_3 = 2\,(p_3 = 0.15)$ (fig. 3*A*). Along two test branches, we simulated an increased intensity of positive selection, with $\omega_3 = 10$, with all other parameters remaining the same (fig. 3*B*).

Results and Discussion

Type I Error Rates

The false positive rate of RELAX is controlled by the significance level of the test. At $P = 0.05$, we rejected the null hypothesis 52 times out of 1,000 replicates in our first set of simulations, placing the estimated type I error rate at 0.052 (95% confidence interval [CI]: 0.040–0.068; Wilson's method).

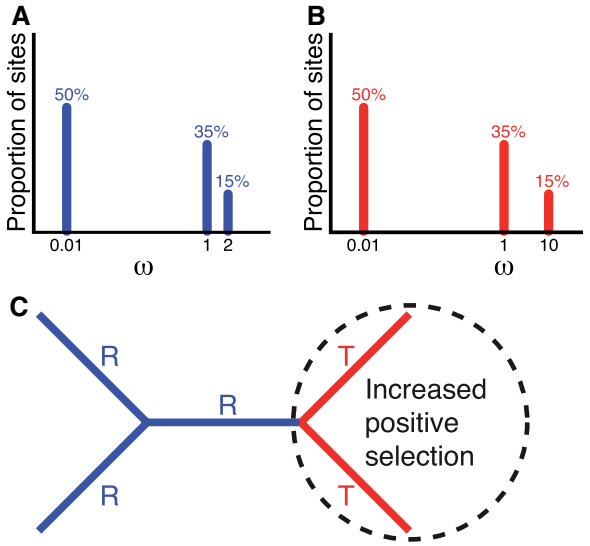

FIG. 3. Simulation strategy to determine if positive selection can be mistaken for relaxation. (*A*) ω distribution for reference branches *R*. (*B*) ω distribution for test branches *T*, in which positive selection (i.e., ω_3) is increased 10-fold relative to the *R* branches. (*C*) Phylogeny over which simulations were performed.

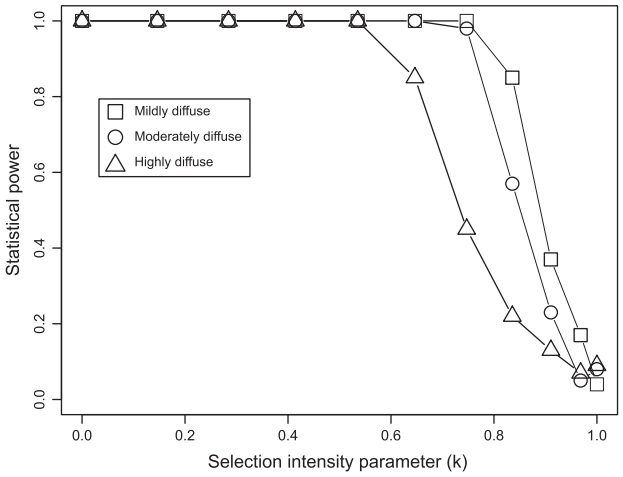

FIG. 4. Power simulations. Circles represent power of RELAX under a mildly diffuse ω distribution: $\omega_1 = 0.1(p_1 = 0.50)$, $\omega_2 = 1.0(p_2 = 0.45)$, $\omega_3 = 2(p_3 = 0.05)$. Triangles represent power of RELAX under a moderately diffuse ω distribution: $\omega_1 = 0.01(p_1 = 0.50)$, $\omega_2 = 1.0(p_2 = 0.45)$, $\omega_3 = 4(p_3 = 0.05)$. Squares represent power of RELAX under a highly diffuse ω distribution: $\omega_1 = 0.001(p_1 = 0.50)$, $\omega_2 = 1.0(p_2 = 0.45)$, $\omega_3 = 8(p_3 = 0.05)$.

Statistical Power

Under all three selection scenarios in our second set of simulations, RELAX had 100% power to detect relaxed selection at $k = 0.5$ (fig. 4). Importantly, these simulated scenarios capture only a tiny fraction of the breadth under which selection may actually operate. Nonetheless, they provide some indication of how large the difference in selective strength between the reference and test branches needs to be for reliable detection by RELAX. In order to quantify the expected power for any given data set, we recommend performing direct power simulations across the phylogeny.

Effect of Increased Positive Selection

Our third set of simulations allowed investigation of whether tests for relaxation that use only a single ω per branch-partition can mislead inference. If ω increases in the test branches due to positive selection, current approaches testing for relaxed selection may detect a different ω closer to 1 and mistakenly infer relaxed selection in the test branches when in fact selection had been intensified (fig. 3). In our simulation, the model with a single ω per branch-partition identified significant differences between test and reference branch ω values in 100/100 simulation replicates (P-value < 0.05). In every case, the estimated reference ω (mean = 0.44) was less than the estimated test ω (mean = 0.64). This result could mistakenly be interpreted as reliable inference of relaxed selection, even though the data were simulated under intensified positive selection. RELAX, by avoiding the unrealistic single-ω assumption, correctly identified intensified selection along test branches in 100/100 replicates, with a mean selection intensity parameter (k) of 3.79. Therefore, RELAX is able to distinguish between an increase in ω due to relaxed selection and an increase in ω due to increased positive selection.

In empirical data sets, we expect the signal for relaxed selection to be driven primarily by sites evolving under purifying rather than positive selection, which are by far the majority. Nevertheless, it is important that a method should not be invalidated by the existence of a small number of positively selected sites.

Bacterial Endosymbionts

Many insect species have obligate (primary) bacterial endosymbionts that perform crucial metabolic processes for the host (Moran and Baumann 2000; McCutcheon et al. 2009; Vogel and Moran 2011). These obligate endosymbionts have arisen multiple times among the γ-proteobacteria (Husník et al. 2011) and are passed vertically from mother to child, thereby introducing convergent features in the bacterial genomes: gene loss, smaller genomes, lower GC content, and reduced thermal stability of proteins (Wernegreen 2002). The effective population size of bacterial endosymbionts is smaller than that of their free-living relatives, partially due to the transmission bottleneck across insect generations (Moran 1996; Funk et al. 2001; Herbeck et al. 2003). Natural selection is less efficient in this setting, and Muller's Ratchet can lead to the accumulation of slightly deleterious mutations (Muller 1964). Accordingly, traces of relaxed selection have been documented in bacterial endosymbionts, including fixation of deleterious alleles (e.g., loss of DNA replication proofreading enzymes) and overall elevated rates of nonsynonymous and radical amino acid replacements (Wernegreen 2011). Insects can also carry facultative (secondary) endosymbionts whose fitness effects on their hosts can be variable and complex (Oliver et al. 2006, 2009; Degnan et al. 2009; Burke et al. 2010). Importantly, because secondary endosymbionts can be transmitted horizontally, we expect them to experience

Table 1. Test for Relaxed Selection Using RELAX in Various Taxonomic Groups.

Taxa	Gene/Genes	Test Branches	Reference Branches	k[a]	*P*-Value
γ-proteobacteria	Single-copy orthologs	Primary/secondary endosymbionts	Free-living γ-proteobacteria	0.30	< 0.0001
		Primary endosymbionts	Free-living γ-proteobacteria	0.28	< 0.0001
		Secondary endosymbionts	Free-living γ-proteobacteria	0.61	< 0.0001
		Primary endosymbionts	Secondary endosymbionts	0.56	< 0.0001
Bats	*SWS1*	HDC echolocating and cave roosting (pseudogenes)	LDC echolocating and tree roosting (functional genes)	0.16	< 0.0001
		LDC echolocating	Tree roosting	1.07	0.577
	M/LWS1	HDC echolocating and cave roosting	LDC echolocating and tree roosting	0.70	0.495
		Echolocating species	Tree- and cave-roosting species	0.21	0.0005
		HDC echolocating	LDC echolocating	0.84	0.427
Bornavirus	Nucleoprotein	Endogenous viral elements	Exogenous virus	0.02	< 0.0001
Daphnia pulex	Mitochondrial protein-coding genes	Asexual	Sexual	0.63	< 0.0001

[a]Estimated selection intensity.

selection which is relaxed relative to the free-living relatives, but intensified relative to the primary endosymbionts, exemplifying an ideal testbed for RELAX applications.

Using RELAX, we find strong evidence for relaxed selection on the 69 single-copy orthologous genes in endosymbiont branches compared with closely related free-living γ-proteobacteria (table 1: $k = 0.30$; P-value < 0.0001). Under the Partitioned Descriptive model with endosymbionts as the test branches and free-living bacteria as reference branches (fig. 5*A*), the pattern of selection conformed to our expectations of relaxed selection, with all ω classes in the test branches shifting toward neutrality (i.e., $\omega = 1$). Specifically, $\omega_{T,1}$, representing the strongest purifying selection, shifted up by an order of magnitude; $\omega_{T,2}$, representing weakly purifying selection shifted from 0.3 to 1.0; and $\omega_{T,3}$, representing positive selection, shifted down by an order of magnitude.

The pattern of relaxation along endosymbiotic lineages is also apparent when we allow each branch to have its own selection intensity parameter (General Descriptive model; fig. 6). The backbone of the phylogeny is under intense selection ($k_b > 1$ shown as red in fig. 6), as are terminal branches leading to free-living γ-proteobacteria, whereas the endosymbiont lineages tend to be more relaxed ($k_b < 1$ shown as blue/purple in fig. 6). This pattern suggests that branch-specific k estimates may provide a guide for describing relaxed selection in the absence of an *a priori* hypothesis. However, we suggest exercising due caution when comparing k_b maximum-likelihood estimates (or any of the other parameter estimates describing the ω distribution) directly, as they are derived from a small volume of information (a single branch) and therefore have high sampling variances (Scheffler et al. 2014). For all of the point estimates of k and ω reported below, it should be borne in mind that our statistical methodology allows us to determine the strength of evidence that k is different from 1 (reported as P-values) but not the sampling variances of the estimates. In particular, high values of ω tend not to be reliably estimable due to flatness of the likelihood surface. Furthermore, the General Descriptive model should not be used to select partitions for formal RELAX hypothesis testing, because it would amount to using the data twice and substantially bias the test result.

Phylogenetic inference that does not account for variable substitution rates arising from skewed GC content found in endosymbionts tends to force their lineages together in a phylogenetic tree, whereas nonhomogeneous models of molecular evolution suggest a larger number of independent origins of endosymbionts from free-living bacteria (Husník et al. 2011). To account for different nucleotide substitution rates within endosymbionts and free-living bacteria, we also performed the analysis under a modified version of RELAX which allowed endosymbionts and free-living bacteria to have separately estimable equilibrium frequencies. This modified test also found strong evidence for relaxed selection in endosymbionts compared with their free-living relatives ($k = 0.33$; P-value < 0.0001). Unlike phylogenetic reconstruction, RELAX does not appear to be misled by systematically skewed GC content, even when this effect is not explicitly modeled, when provided with an accurate phylogeny.

We also investigated the patterns of selection in primary and secondary endosymbionts separately (table 1 and fig. 5*B*–*D*) using the Partitioned Descriptive model and the RELAX test. Relative to free-living bacteria, there was sufficient signal to detect relaxation in both primary endosymbionts ($k = 0.28$; P-value < 0.0001) and secondary endosymbionts ($k = 0.61$; P-value < 0.0001) independently. Moreover, primary endosymbiont lineages evolved under relaxed selection compared with secondary endosymbionts ($k = 0.56$; P-value < 0.0001). This pattern was expected since primary endosymbionts likely experience tighter bottlenecks during vertical transmission and their genomes show greater evidence of extreme evolutionary features (e.g., gene loss and AT bias; McCutcheon and Moran 2012).

Opsin Genes in Bats

The loss of vision in animals that reside in total darkness (e.g., cave-dwelling fish) is a classic case of trait loss caused by relaxed selection (Darwin 1859). Correspondingly, the importance of color vision is likely reduced in nocturnal animals

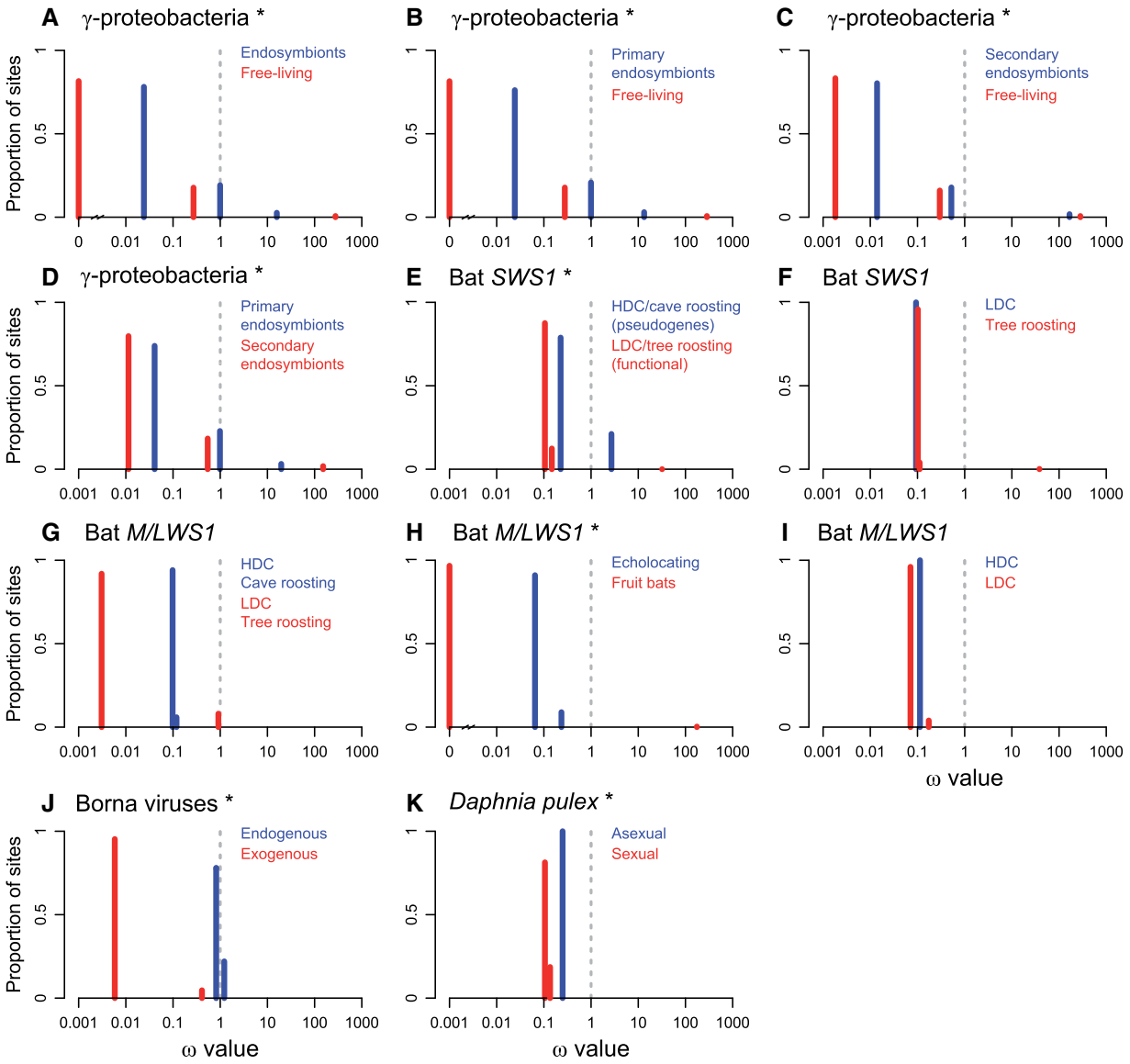

Fig. 5. Patterns of natural selection across taxonomic groups under the Partitioned Descriptive model. Selection profiles for (*A*–*D*) concatenated genes from the γ-proteobacteria, (*E* and *F*) *SWS1* in echolocating and fruit bats, (*G*–*I*) *M/LWS1* in echolocating and fruit bats, (*J*) Borna virus nucleoprotein and EBLN elements, and (*K*) *Daphnia pulex* mitochondrial protein-coding regions are shown. Three ω parameters and the relative proportion of sites they represent are plotted for test (blue) and reference (red) branches. Only ω categories representing nonzero proportions of sites are shown. The gray vertical dashed line at $\omega = 1$ represents neutral evolution. Asterisks indicate significant relaxation ($P < 0.05$) between test and reference branches (see table 1).

(Zhao, Rossiter, et al. 2009; Veilleux et al. 2013). For instance, in fruit bats (Yinpterochiroptera) and echolocating bats (Yangochiroptera), the short-wavelength-sensitive (*SWS1*) gene, associated with blue–violet color vision, has been lost in some species. Fruit bats do not echolocate (with a few exceptions, not represented in our data set) and can be subdivided into cave-roosting and tree-roosting species. Echolocating bats can be subdivided into high duty cycle (HDC) and low duty cycle (LDC) echolocating species. HDC echolocation involves emitting calls of long duration with short intervals between calls and may enhance hunting ability (Fenton et al. 2012). The *SWS1* gene has been lost in cave-roosting fruit bats and HDC echolocating species, but functional *SWS1* genes have been maintained in tree-roosting and LDC echolocating species. In HDC echolocating bats, the loss of *SWS1* may be a result of a trade-off between vision and hearing (Speakman 2001), whereas in cave-roosting fruit bats it may simply reflect the poor light conditions in caves which make color hues more difficult to discern.

Using RELAX, we found strong evidence that selection on *SWS1* was relaxed in bat species in which this gene had become pseudogenized (cave-roosting and HDC echolocating species) (table 1: $k = 0.16$; P-value < 0.0001). Once a gene has lost functionality, purifying selection is expected to abate: this hypothesis is confirmed by the inferred reduction in the relative strength of both purifying and positive selection in the *SWS1* pseudogenes in cave-roosting and HDC echolocating species (fig. 5*E*). We did not, however, infer a perfectly neutral mode ($\omega = 1$) for these pseudogenes, because *SWS1* was likely still functional in part of the phylogeny prior to

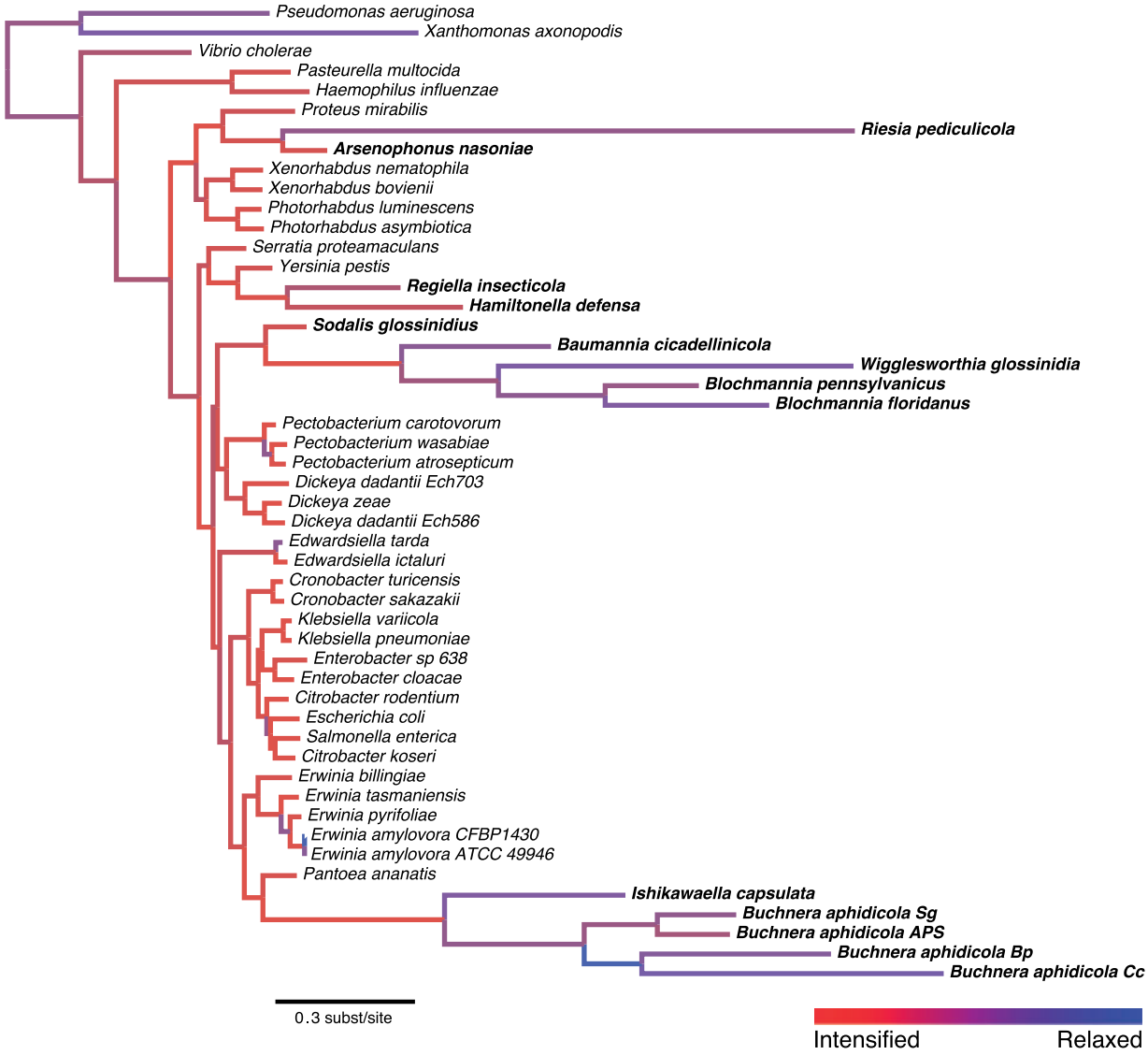

Fig. 6. Branch specific relaxation parameters inferred for the γ-proteobacteria phylogeny under the General Descriptive model. Branches are colored based on relative value of the selection intensity parameter k_b (red for large values and blue for small values). Primary and secondary endosymbiont taxa are labeled in bold text.

pseudogenization. When we compared the intensity of selection among species whose *SWS1* gene did not undergo pseudogenization (LDC echolocating vs. tree-roosting species), we found no significant difference (table 1: $k = 1.07$; *P*-value = 0.577; fig. 5*F*). This finding suggests that the evolution of echolocation itself does not imply relaxed selection on *SWS1*.

A second opsin gene involved in green–red vision, medium/long wavelength sensitive (*M/LWS1*), has been retained across all documented bat species. Zhao, Rossiter, et al. (2009) inferred lineage-specific ω values and consistent patterns of purifying selection (ω ranging between 0.0 and 0.48). Similarly, we found that the pattern of relaxed selection in HDC echolocating and cave-roosting bats observed in *SWS1* does not hold in *M/LWS1* (table 1: $k = 0.70$; *P*-value = 0.495; fig. 5*G*). However, when we compared the intensity of selection in echolocating species to that in tree and cave roosting fruit bat species, we found evidence of relaxed selection in the echolocating species (table 1: $k = 0.21$; *P*-value = 0.0005; fig. 5*H*). Moreover, there was no difference in the intensity of selection between species with different types of echolocation (table 1: $k = 0.84$; *P*-value = 0.427; fig. 5*I*). This relaxation of selection in all echolocating species, over tens of millions of years, has not led to the formation of *M/LWS1* pseudogenes in the echolocating species, which suggests some functionality of this gene may have been retained. Indeed, it has been suggested that color vision proteins may be involved in regulating circadian rhythms (Nei et al. 1997; Nemec et al. 2008).

Endogenous Viral Elements

Despite a reputation for rapid adaptive evolution, exogenous free-living RNA viruses are subject to remarkably strong purifying selection (Holmes 2003; Pybus et al. 2007; Wertheim and Kosakovsky Pond 2011). These selective constraints likely arise from the necessity to encode genes for complex biological functions in compact genomes. However, some

exogenous RNA viruses have become permanently integrated into their hosts' genomes (Belyi et al. 2010). Upon integration, these endogenous viral elements are presumably freed from most selective constraints, because they cannot produce replication-competent viruses.

Borna disease viruses may have integrated into mammalian genomes over 65 Ma (Horie et al. 2013). The virus has also experienced more recent endogenization events, such as the integration into the 13-lined ground squirrel genome. As expected, we found that the endogenized elements experienced relaxed selection relative to their exogenous counterparts (table 1: $k = 0.02$; P-value < 0.0001; fig. 5*J*). If the endogenous viral elements were not subject to any level of purifying selection at the amino acid level, one would expect all the sites to evolve under an ω equal to 1. We inferred 78% of the sites evolved under an ω of 0.82, with the remaining 22% evolving under $\omega = 1.2$. The small deviation from neutrality may be driven by the components of these branches preceding viral endogenization.

Sexual versus Asexual Reproduction

The ultimate reasons for the evolution of sexual reproduction remain obscure. From an evolutionary perspective, sexual reproduction is costly (Maynard Smith 1978); however, asexual animal species are rare and typically do not persist for long periods of time (Barton 2009). This observation has been attributed to the hypothesis that asexual reproduction can lead to lower efficiency of selection due to an increase in linkage disequilibrium. Mitochondria are not part of the sexually reproducing genome, but they should experience the selective effects of a transition from sexuality to asexuality (Paland and Lynch 2006). After the transition to asexuality, there is no longer segregation between the nuclear and mitochondrial genomes, and the mitochondrial and nuclear genomes are in complete linkage disequilibrium. Therefore, one would expect an excess of mildly deleterious mutations accumulating in mitochondrial genomes due to relaxed selection in asexual lineages.

In the asexual microcrustacean *Daphnia pulex*, we found mitochondrial protein-coding regions to be under relaxed selective constraints compared with the sexual *D. pulex* branches (table 1: $k = 0.63$; P-value = 0.00003; fig. 5*K*). In the sexual branches, 81% of the sites were explained by an ω of 0.11 and the remaining 19% of sites were explained by an ω of 0.14. In the asexual branches, 100% of sites evolved under a single $\omega = 0.25$. In this instance, RELAX is in concordance with the analysis performed by Paland and Lynch (2006), who found an increase in ω in the asexual *D. pulex* lineages.

Recently, Tucker et al. (2013) examined the genomes of sexual and asexual *D. pulex* lineages and found evidence for more recent transitions to asexuality, on the order of decades. This finding is at odds with the mutation accumulation hypothesis, described earlier, for increased ω in these asexual lineages. If the hypothesis put forth by Tucker et al. (2013) is correct, there would be no *a priori* reason to expect relaxation in lineages leading to asexual *D. pulex*. Our analysis cannot resolve this discrepancy, though our findings suggest that the relative intensity of natural selection tends to differ in *D. pulex* lineages in which asexuality arises.

Conclusions

We developed a formal test for detecting relaxation or intensification of selective pressures in a comparative phylogenetic framework. RELAX assesses whether selective strength on the test subset of branches is compressed toward or repelled away from neutrality, relative to the reference subset of branches. Unlike previous approaches used to detect relaxed selection, RELAX does not mistake intensified positive selection for relaxed purifying selection.

We demonstrated that RELAX is well behaved on simulated data and established its power to detect relaxed selection via simulation and in four biological systems predicted to exhibit changes in the intensity of selection on a subset of branches. In all four biological systems, RELAX was able to detect relaxation of selective pressures where it had been predicted by evolutionary theory and in concordance with previous studies. In the clearest scenario comparing pseudogenes with functional genes (e.g., endogenous viruses and opsin genes in nocturnal animals), RELAX confidently identified significant relaxation on pseudogene branches. In addition, RELAX analysis confirmed that populations with reduced effective population sizes (e.g., bacterial endosymbionts and recently emerged asexual lineages) experienced selective relaxation compared with their close relatives that have larger effective population sizes. RELAX was also able to distinguish between degrees of relaxation in obligate versus facultative bacterial endosymbionts.

A caveat of phylogenetic methods in general is that sequence data are uninformative regarding changes that happen at subbranch timescales and consequently that changes in selective pressure over short timescales are difficult to characterize. For instance, if episodic positive selection acts so fast that there is a switch from purifying selection to positive selection and back to purifying selection along a single branch of the tree, the effect would be to increase the average ω value inferred for that branch. If the increased ω value remains below 1, the overall effect on the observed sequences would be indistinguishable from that of relaxation. In the phylogenetic framework, this issue can only be circumvented by sampling more sequences.

Nonetheless, RELAX holds the potential to find evidence of relaxed selection where it might not be obvious based on evolutionary theory. For example, the evidence of relaxed selection within the bat opsin gene *M/LWS1*, that has not degraded into pseudogenes in any sampled lineage, bolsters the hypothesis that this gene has an important secondary function. This result exemplifies the biological questions that can be explored using this powerful new approach for detecting relaxed selection.

Materials and Methods

Empirical Data Sets

1) The γ-proteobacteria data set comprises a concatenated alignment of 69 single-copy, orthologous genes from 50

bacterial species assembled and aligned by Husník et al. (2011). These genes were typically conserved and involved in translation, ribosomal structure, and biogenesis. The endosymbiotic γ-proteobacteria tend to artificially cluster in phylogenic inference due to their exceptionally low GC-content. This bias can be corrected by using nonhomogeneous nucleotide substitution models in phylogenetic inference (Galtier and Gouy 1995, 1998). Therefore, we used a phylogeny inferred by Husník et al. (2011), who used this type of nucleotide model in their analysis.

2) Two bat opsin genes, *SWS1* and *M/LWS1*, were previously investigated by Zhao, Rossiter, et al. (2009) for evidence of relaxed selection. We aligned each gene separately using MUSCLE and constructed maximum-likelihood phylogenies using the GTR + Γ_4 model in PhyML v3.0, implemented in SeaView (Edgar 2004; Gouy et al. 2010; Guindon et al. 2010). Insertions and deletions in SWS1 pseudogenes that resulted in frameshifts were excised to maintain codon structure.
3) Borna disease virus nucleoprotein genes, avian bornavirus nucleoprotein genes, endogenous bornavirus-like nucleoprotein-2 (EBLN-2) elements in primates, and a homologous region in the 13-lined ground squirrel genome identified by Horie et al. (2010) were downloaded from GenBank. These sequences were aligned using MUSCLE and a maximum-likelihood phylogeny was constructed using the GTR + Γ_4 model in PhyML. Insertions and deletions in EBLN-2 elements that resulted in frameshifts were excised to maintain codon structure.
4) Protein-coding regions from complete mitochondrial genomes from 27 *D. pulex* strains (both sexual and asexual lineages) were aligned using MUSCLE, along with two *D. melanica* isolates which served as an outgroup. A maximum-likelihood phylogeny was inferred using the GTR + Γ_4 model in PhyML.

The data set sizes and the run times for analyzing them are summarized in supplementary table S1, Supplementary Material online. All alignments and phylogenies are available as NEXUS files as supplementary material S1, Supplementary Material online, and at http://bit.ly/veg_manuscripts_relax.

Implementation

The four models and the RELAX test have been implemented in an interactive HyPhy Batch Language file as the RELAX.bf standard analysis available in the current HyPhy (Pond et al. 2005) source distribution, v2.2, https://github.com/veg/hyphy, and is available on the Datamonkey webserver at www.datamonkey.org/RELAX (Pond and Frost 2005; Delport et al. 2010).

Supplementary Material

Supplementary material S1 and table S1 is available at *Molecular Biology and Evolution* online (http://www.mbe.oxfordjournals.org/).

Acknowledgments

This research was supported in part by the National Institutes of Health (AI110181, AI090970, AI100665, DA034978, GM093939, U54HL108460, U01GM110749), the UCSD Center for AIDS Research Developmental Grant (AI36214), Bioinformatics and Information Technologies Core, the International AIDS Vaccine Initiative (AI090970), the UC Laboratory Fees Research Program grant 12-LR-236617, and the National Research Foundation of South Africa. The authors thank Steven Weaver for his assistance in the online implementation of RELAX.

References

Anisimova M, Kosiol C. 2009. Investigating protein-coding sequence evolution with probabilistic codon substitution models. *Mol Biol Evol.* 26(2):255–271.
Barton NH. 2009. Why sex and recombination? *Cold Spring Harb Symp Quant Biol.* 74:187–195.
Belyi VA, Levine AJ, Skalka AM. 2010. Unexpected inheritance: multiple integrations of ancient bornavirus and ebolavirus/marburgvirus sequences in vertebrate genomes. *PLoS Pathog.* 6(7):e1001030.
Bielawski JP, Yang Z. 2003. Maximum likelihood methods for detecting adaptive evolution after gene duplication. *J Struct Funct Genomics.* 3(1-4):201–212.
Burke G, Fiehn O, Moran N. 2010. Effects of facultative symbionts and heat stress on the metabolome of pea aphids. *ISME J.* 4(2):242–252.
Dainat J, Paganini J, Pontarotti P, Gouret P. 2012. GLADX: an automated approach to analyze the lineage-specific loss and pseudogenization of genes. *PLoS One* 7(6):e38792.
Darwin C. 1859. On the origin of species by means of natural selection. *J. Murray* London.
Degnan PH, Yu Y, Sisneros N, Wing RA, Moran NA. 2009. *Hamiltonella defensa*, genome evolution of protective bacterial endosymbiont from pathogenic ancestors. *Proc Natl Acad Sci U S A.* 106(22):9063–9068.
Delport W, Poon AFY, Frost SDW, Kosakovsky Pond SL. 2010. Datamonkey. 2010: a suite of phylogenetic analysis tools for evolutionary biology. *Bioinformatics* 26(19):2455–2457.
Delport W, Scheffler K, Seoighe C. 2009. Models of coding sequence evolution. *Brief Bioinform.* 10(1):97–109.
Edgar RC. 2004. MUSCLE: multiple sequence alignment with high accuracy and high throughput. *Nucleic Acids Res.* 32(5):1792–1797.
Elde NC, Malik HS. 2009. The evolutionary conundrum of pathogen mimicry. *Nat Rev Microbiol.* 7(11):787–797.
Eyre-Walker A. 2006. The genomic rate of adaptive evolution. *Trends Ecol Evol.* 21(10):569–575.
Felsenstein J. 1981. Evolutionary trees from DNA sequences: a maximum likelihood approach. *J Mol Evol.* 17(6):368–376.
Feng P, Zheng J, Rossiter SJ, Wang D, Zhao H. 2014. Massive losses of taste receptor genes in toothed and baleen whales. *Genome Biol Evol.* 6(6):1254–1265.
Fenton MB, Faure PA, Ratcliffe JM. 2012. Evolution of high duty cycle echolocation in bats. *J Exp Biol.* 215(Pt 17):2935–2944.
Funk DJ, Wernegreen JJ, Moran NA. 2001. Intraspecific variation in symbiont genomes: bottlenecks and the aphid-buchnera association. *Genetics* 157(2):477–489.
Galtier N, Gouy M. 1995. Inferring phylogenies from DNA sequences of unequal base compositions. *Proc Natl Acad Sci U S A.* 92(24):11317–11321.
Galtier N, Gouy M. 1998. Inferring pattern and process: maximum-likelihood implementation of a nonhomogeneous model of DNA sequence evolution for phylogenetic analysis. *Mol Biol Evol.* 15(7):871–879.

Go Y, Satta Y, Takenaka O, Takahata N. 2005. Lineage-specific loss of function of bitter taste receptor genes in humans and nonhuman primates. *Genetics* 170(1):313–326.
Goldman N, Yang Z. 1994. A codon-based model of nucleotide substitution for protein-coding DNA sequences. *Mol Biol Evol.* 11(5):725–736.
Gouy M, Guindon S, Gascuel O. 2010. SeaView version 4: a multiplatform graphical user interface for sequence alignment and phylogenetic tree building. *Mol Biol Evol.* 27(2):221–224.
Graur D, Zheng Y, Price N, Azevedo RBR, Zufall RA, Elhaik E. 2013. On the immortality of television sets: "function" in the human genome according to the evolution-free gospel of ENCODE. *Genome Biol Evol.* 5(3):578–590.
Guindon S, Dufayard J-F, Lefort V, Anisimova M, Hordijk W, Gascuel O. 2010. New algorithms and methods to estimate maximum-likelihood phylogenies: assessing the performance of PhyML 3.0. *Syst Biol.* 59(3):307–321.
Herbeck JT, Funk DJ, Degnan PH, Wernegreen JJ. 2003. A conservative test of genetic drift in the endosymbiotic bacterium Buchnera: slightly deleterious mutations in the chaperonin groEL. *Genetics* 165(4):1651–1660.
Holmes EC. 2003. Patterns of intra- and interhost nonsynonymous variation reveal strong purifying selection in dengue virus. *J Virol.* 77(20):11296–11298.
Holmes EC, Drummond AJ. 2007. The evolutionary genetics of viral emergence. *Curr Top Microbiol Immunol.* 315:51–66.
Horie M, Honda T, Suzuki Y, Kobayashi Y, Daito T, Oshida T, Ikuta K, Jern P, Gojobori T, Coffin JM, et al. 2010. Endogenous non-retroviral RNA virus elements in mammalian genomes. *Nature* 463(7277):84–87.
Horie M, Kobayashi Y, Suzuki Y, Tomonaga K. 2013. Comprehensive analysis of endogenous bornavirus-like elements in eukaryote genomes. *Philos Trans R Soc Lond B Biol Sci.* 368(1626):20120499.
Hunt BG, Ometto L, Wurm Y, Shoemaker D, Yi SV, Keller L, Goodisman MAD. 2011. Relaxed selection is a precursor to the evolution of phenotypic plasticity. *Proc Natl Acad Sci U S A.* 108(38):15936–15941.
Husník F, Chrudimský T, Hypša V. 2011. Multiple origins of endosymbiosis within the Enterobacteriaceae (γ-Proteobacteria): convergence of complex phylogenetic approaches. *BMC Biol.* 9:87.
Kosakovsky Pond S, Delport W, Muse SV, Scheffler K. 2010. Correcting the bias of empirical frequency parameter estimators in codon models. *PLoS One* 5(7):e11230.
Kosakovsky Pond SL, Murrell B, Fourment M, Frost SDW, Delport W, Scheffler K. 2011. A random effects branch-site model for detecting episodic diversifying selection. *Mol Biol Evol.* 28(11) 3033–3043.
Kosakovsky Pond SL, Scheffler K, Gravenor MB, Poon AFY, Frost SDW. 2010. Evolutionary fingerprinting of genes. *Mol Biol Evol.* 27(3):520–536.
Lahti DC, Johnson NA, Ajie BC, Otto SP, Hendry AP, Blumstein DT, Coss RG, Donohue K, Foster SA. 2009. Relaxed selection in the wild. *Trends Ecol Evol.* 24(9):487–496.
Lenski RE, Ofria C, Pennock RT, Adami C. 2003. The evolutionary origin of complex features. *Nature* 423(6936):139–144.
Lynch M, Conery JS. 2000. The evolutionary fate and consequences of duplicate genes. *Science* 290(5494):1151–1155.
Marková S, Searle JB, Kotlík P. 2014. Relaxed functional constraints on triplicate α-globin gene in the bank vole suggest a different evolutionary history from other rodents. *Heredity* 113(1):64–73.
Maynard Smith J. 1978. The evolution of sex. Cambridge: Cambridge University Press.
McCutcheon JP, McDonald BR, Moran NA. 2009. Convergent evolution of metabolic roles in bacterial co-symbionts of insects. *Proc Natl Acad Sci U S A.* 106(36):15394–15399.
McCutcheon JP, Moran NA. 2012. Extreme genome reduction in symbiotic bacteria. *Nat Rev Microbiol.* 10(1):13–26.
Moran NA. 1996. Accelerated evolution and Muller's Rachet in endosymbiotic bacteria. *Proc Natl Acad Sci U S A.* 93(7):2873–2878.
Moran NA, Baumann P. 2000. Bacterial endosymbionts in animals. *Curr Opin Microbiol.* 3(3):270–275.
Muller HJ. 1964. The relation of recombination to mutational advance. *Mutat Res.* 106:2–9.
Murrell B, Wertheim JO, Moola S, Weighill T, Scheffler K, Kosakovsky Pond SL. 2012. Detecting individual sites subject to episodic diversifying selection. *PLoS Genet.* 8(7):e1002764.
Muse SV, Gaut BS. 1994. A likelihood approach for comparing synonymous and nonsynonymous nucleotide substitution rates, with application to the chloroplast genome. *Mol Biol Evol.* 11(5):715–724.
Nei M, Zhang J, Yokoyama S. 1997. Color vision of ancestral organisms of higher primates. *Mol Biol Evol.* 14(6):611–618.
Nemec P, Cveková P, Benada O, Wielkopolska E, Olkowicz S, Turlejski K, Burda H, Bennett NC, Peichl L. 2008. The visual system in subterranean African mole-rats (Rodentia, Bathyergidae): retina, subcortical visual nuclei and primary visual cortex. *Brain Res Bull.* 75(2–4):356–364.
Nielsen R, Yang Z. 1998. Likelihood models for detecting positively selected amino acid sites and applications to the HIV-1 envelope gene. *Genetics* 148(3):929–936.
Ohno S. 1970. Evolution by gene duplication. New York: Allen and Unwin.
Oliver KM, Degnan PH, Hunter MS, Moran NA. 2009. Bacteriophages encode factors required for protection in a symbiotic mutualism. *Science* 325(5943):992–994.
Oliver KM, Moran NA, Hunter MS. 2006. Costs and benefits of a superinfection of facultative symbionts in aphids. *Proc Biol Sci.* 273(1591):1273–1280.
Paland S, Lynch M. 2006. Transitions to asexuality result in excess amino acid substitutions. *Science* 311(5763):990–992.
Pond SLK, Frost SDW. 2005. Datamonkey: rapid detection of selective pressure on individual sites of codon alignments. *Bioinformatics* 21(10):2531–2533.
Pond SLK, Frost SDW, Grossman Z, Gravenor MB, Richman DD, Brown AJL. 2006. Adaptation to different human populations by HIV-1 revealed by codon-based analyses. *PLoS Comput Biol.* 2(6):e62.
Pond SLK, Frost SDW, Muse SV. 2005. HyPhy: hypothesis testing using phylogenies. *Bioinformatics* 21(5):676–679.
Pybus OG, Rambaut A, Belshaw R, Freckleton RP, Drummond AJ, Holmes EC. 2007. Phylogenetic evidence for deleterious mutation load in RNA viruses and its contribution to viral evolution. *Mol Biol Evol.* 24(3):845–852.
Scheffler K, Murrell B, Kosakovsky Pond SL. 2014. On the validity of evolutionary models with site-specific parameters. *PLoS One* 9(4):e94534.
Snell-Rood EC, Van Dyken JD, Cruickshank T, Wade MJ, Moczek AP. 2010. Toward a population genetic framework of developmental evolution: the costs, limits, and consequences of phenotypic plasticity. *Bioessays* 32(1):71–81.
Speakman JR. 2001. The evolution of flight and echolocation in bats: another leap in the dark. *Mamm Rev.* 31(2):111–130.
Templeton AR. 2008. The reality and importance of founder speciation in evolution. *Bioessays* 30(5):470–479.
Tucker AE, Ackerman MS, Eads BD, Xu S, Lynch M. 2013. Population-genomic insights into the evolutionary origin and fate of obligately asexual *Daphnia pulex*. *Proc Natl Acad Sci U S A.* 110(39):15740–15745.
Veilleux CC, Louis EE Jr, Bolnick DA. 2013. Nocturnal light environments influence color vision and signatures of selection on the OPN1SW opsin gene in nocturnal lemurs. *Mol Biol Evol.* 30(6):1420–1437.
Vogel KJ, Moran NA. 2011. Sources of variation in dietary requirements in an obligate nutritional symbiosis. *Proc Biol Sci.* 278(1702):115–121.
Wernegreen JJ. 2002. Genome evolution in bacterial endosymbionts of insects. *Nat Rev Genet.* 3(11):850–861.
Wernegreen JJ. 2011. Reduced selective constraint in endosymbionts: elevation in radical amino acid replacements occurs genome-wide. *PLoS One* 6(12):e28905.

Wertheim JO, Kosakovsky Pond SL. 2011. Purifying selection can obscure the ancient age of viral lineages. *Mol Biol Evol.* 28(12):3355–3365.

Wertheim JO, Worobey M. 2009. Relaxed selection and the evolution of RNA virus mucin-like pathogenicity factors. *J Virol.* 83(9):4690–4694.

Wicke S, Schäferhoff B, dePamphilis CW, Müller KF. 2014. Disproportional plastome-wide increase of substitution rates and relaxed purifying selection in genes of carnivorous Lentibulariaceae. *Mol Biol Evol.* 31(3):529–545.

Wu CI, Li WH, Shen JJ, Scarpulla RC, Limbach KJ, Wu R. 1986. Evolution of cytochrome c genes and pseudogenes. *J Mol Evol.* 23(1):61–75.

Yang Z, Nielsen R. 2002. Codon-substitution models for detecting molecular adaptation at individual sites along specific lineages. *Mol Biol Evol.* 19(6):908–917.

Yang Z, Nielsen R, Goldman N, Pedersen AM. 2000. Codon-substitution models for heterogeneous selection pressure at amino acid sites. *Genetics* 155(1):431–449.

Zhao H, Rossiter SJ, Teeling EC, Li C, Cotton JA, Zhang S. 2009. The evolution of color vision in nocturnal mammals. *Proc Natl Acad Sci U S A.* 106(22):8980–8985.

Zhao H, Ru B, Teeling EC, Faulkes CG, Zhang S, Rossiter SJ. 2009. Rhodopsin molecular evolution in mammals inhabiting low light environments. *PLoS One* 4(12):e8326.